Published in final edited form as:

Acta Biomater. 2017 March 01; 50: 546–555. doi:10.1016/j.actbio.2016.12.039.

Ex vivo blood vessel bioreactor for analysis of the biodegradation of magnesium stent models with and without vessel wall integration

Juan Wang[a,c,1], **Lumei Liu**[a,b,1], **Yifan Wu**[d], **Manfred F. Maitz**[e], **Zhihong Wang**[d], **Youngmi Koo**[a,b], **Ansha Zhao**[c], **Jagannathan Sankar**[a,b], **Deling Kong**[d,*], **Nan Huang**[c,*], and **Yeoheung Yun**[a,b,*]

[a]NSF Engineering Research Center for Revolutionizing Metallic Biomaterials, North Carolina A&T State University, Greensboro, NC 27411, USA

[b]FIT BEST Laboratory, Department of Chemical, Biological, and Bio Engineering, North Carolina A&T State University, Greensboro, NC 27411, USA

[c]Key Laboratory of Advanced Technologies of Materials, Ministry of Education, School of Materials Science and Engineering, Southwest Jiaotong University, Chengdu, Sichuan 610031, PR China

[*]Corresponding authors at: NSF Engineering Research Center for Revolutionizing Metallic Biomaterials, FIT BEST Laboratory, Department of Chemical, Biological, and Bio Engineering, North Carolina A&T State University, Greensboro, NC 27411, USA (Y. Yun). Key Laboratory of Advanced Technologies of Materials, Ministry of Education, School of Materials Science and Engineering, Southwest Jiaotong University, Chengdu, Sichuan 610031, PR China (N. Huang). State Key Laboratory of Medicinal Chemical Biology, Key Laboratory of Bioactive Materials, Ministry of Education, Nankai University, Tianjin 300071, PR China (D. Kong), kongdeling@nankai.edu.cn (D. Kong), huangnan1956@163. com (N. Huang), yyun@ncat.edu (Y. Yun).

[1]These authors contributed equally to this work.

Disclosure

The authors state that they have no conflicts of interest.

Contributors

- Juan Wang, who is the first author in this manuscript, designed this idea, conducted all the tests, analyzed all the data and prepared the manuscript.
- Lumei Liu conducted *in vitro* and ex vivo tests, and prepared the manuscript. She contributed equally to this work with the first author.
- Yifan Wu conducted *in vivo* test.
- Manfred F. Maitz discussed actively on original idea on ex vivo vascular bioreactor and polished the manuscript.
- Zhihong Wang designed *in vivo* test.
- Youngmi Koo helped to set up the ex vivo vascular bioreactor.
- Ansha Zhao positively discussed on the *in vivo* data.
- Jagannathan Sankar, who is the director of our research center, provided the funding for ex vivo test.
- Deling Kong, who is one of corresponding authors in this manuscript, provided the idea and experimental platform of *in vivo* test.
- Nan Huang is one of corresponding authors in this manuscript, and he is the first author's advisor. In this work, he advised the design of the tests and the discussion.
- Yeoheung Yun is the first corresponding author in this manuscript, and he is the first author's co-advisor. In this work, he managed all the tests and co-authors as well as advised the structure and details of the manuscript.

[d]State Key Laboratory of Medicinal Chemical Biology, Key Laboratory of Bioactive Materials, Ministry of Education, Nankai University, Tianjin 300071, PR China

[e]Leibniz Institute of Polymer Research Dresden, Max Bergmann Center of Biomaterials Dresden, Dresden 01069, Germany

Abstract

Current *in vitro* models fail in predicting the degradation rate and mode of magnesium (Mg) stents *in vivo*. To overcome this, the microenvironment of the stent is simulated here in an *ex vivo* bioreactor with porcine aorta and circulating medium, and compared with standard static *in vitro* immersion and with *in vivo* rat aorta models. In *ex vivo* and *in vivo* conditions, pure Mg wires were exposed to the aortic lumen and inserted into the aortic wall to mimic early- and long-term implantation, respectively. Results showed that: 1) Degradation rates of Mg were similar for all the fluid diffusion conditions (*in vitro* static, aortic wall *ex vivo* and *in vivo*); however, Mg degradation under flow condition (i.e. in the lumen) *in vivo* was slower than *ex vivo*; 2) The corrosion mode in the samples can be mainly described as localized (*in vitro*), mixed localized and uniform (*ex vivo*), and uniform (*in vivo*); 3) Abundant degradation products ($MgO/Mg(OH)_2$ and Ca/P) with gas bubbles accumulated around the localized degradation regions *ex vivo*, but a uniform and thin degradation product layer was found *in vivo*. It is concluded that the *ex vivo* vascular bioreactor provides an improved test setting for magnesium degradation between static immersion and animal experiments and highlights its promising role in bridging degradation behavior and biological response for vascular stent research.

Keywords

Magnesium; Biodegradation; Vascular bioreactor; *Ex vivo*; *In vitro*; *In vivo*

1. Introduction

Magnesium (Mg) and its alloys have received considerable attention as candidates for a new generation of biodegradable stent materials [1,2]. For example, absorbable Mg-based stents have been tested in various *in vitro* environments to evaluate their biosafety in vascular applications [3,4]. Meanwhile, they have been studied for several years in animal and clinical trials with encouraging results [5,6]. However, the degradation behavior tested in *in vitro* is not comparable with that in *in vivo* and there are obvious differences between *in vitro* and *in vivo* degradation rates and modes [7]. Although in 2014 ISO/TS 17137 has suggested extracorporeal and pre-clinical *in vivo* concepts to evaluate cardiovascular absorbable implants, no recommended method currently exists for *in vitro* analysis of the degradation behavior of absorbable metals to predict the *in vivo* situation due to the different test conditions and the complex reactions at the implant-tissue interface [8]. Up to now, there is an ongoing discussion about the reliability and predictability of the applied *in vitro* methods [9]. The challenges to build the systematic test system include i) the lack of *in vitro* models that sufficiently mimic the *in vivo* conditions [10]; ii) insufficient understanding of the factors that influence degradation behavior of Mg-based materials *in vitro*, which are keys to predict *in vivo* degradation [11]; and iii) a paucity of thorough knowledge of

degradation mechanisms *in vivo*. The accurate determination of the degradation of bio-absorbable metals is a technologically important issue in science and biomedical applications [12]. A key step to develop current standards is to identify and test the biological, biochemical and biophysical microenvironment and develop parameters in test-systems for the specific applications.

Every medical device undergoes an interaction with the bioenvironment, in which its surface is exposed to organic [4] and inorganic [13] constituents, followed by a complex molecular, blood [3], cell [14] and tissue response [15]. Also, the fluid dynamics [16], gas supply and diffusion [4], pH [17] and temperature have impact on the degradation [18]. This "physiological degradation" was defined by Willumeit et al. to describe degradation under cell culture conditions and the relevance of the influencing factors was determined by neural network analysis [19]. The degradation of a stent causes ion release and pH change, which in turn affect the host cell and biological microenvironment. Furthermore, the parameters from the complex remodeling of the vascular microenvironment critically influence the degradation behavior of absorbable stents. That is, the biodegradation behavior is modified by different microenvironments at the early- and long-term implantation process (i.e. the stages before and after endothelialization). In the physiologically hydrodynamic vascular system, the stent is exposed to the blood before the endothelialization on the stent. The fluid shear force acting on the vessel wall is transduced into biochemical and biophysical signals, leading to various degradation behaviors. In our previous studies, a couple of *in vitro* bioreactors, such as the varied flow bioreactor with computational fluid dynamic calculation [16] and an *in-situ* and *real-time* electrochemical monitoring bioreactor [20], have been developed to simulate the *in vivo* conditions and to reveal the biodegradation behavior and mechanism of Mg-based alloys and stents. It was demonstrated that the fluid flow has a significant impact on the degradation of absorbable metallic stents, including degradation kinetics, degradation modes, degradation rates, degradation products, and local pH changes [21,16]. After the stent is covered by neointima [22], it is no longer exposed to flow and degradation is dominated by diffusion of water, hydrophilic solutes and ions between vascular tissue and the stent. Besides hydrodynamics, the tissue response is also a vital factor to affect the degradation behavior of Mg-based stents [23]. For simulation of the degradation, it is of fundamental concern to control the *in vitro* environment in a way that approximates the *in vivo* physiological conditions during the early- and long-term implantation process [19].

Due to the complexity of the arterial wall structure and the difficulty to grow an artery *in vitro*, it is challenging to build an *in vitro* simulation model of this case. Therefore, investigation of a real artery cultured in a perfusion bioreactor might be a promising approach to provide a more simulated vascular environment. In this study, an *ex vivo* aorta model using a vascular bioreactor was developed to study Mg biodegradation. Results are systematically compared with *in vitro* standard immersion and *in vivo* assessments. This bioreactor was expected to determine Mg degradation behavior in more accurate parameters than the *in vitro* assay, for a better understanding of the *in vivo* degradation behavior of Mg-based stents.

2. Materials and methods

2.1. Pure magnesium wires preparation

As-drawn magnesium wire of 99.9% purity purchased from Goodfellow USA (Coraopolis, PA) was used as Mg implants. Impurities included <1 ppm Ag, 10 ppm Ca, 5 ppm Cu, <1 ppm Na, 100 ppm Si, and 100 ppm Fe. Samples were polished with 1200 grit abrasive paper, using isopropanol as a lubricant. The diameter of the wire was 250 ± 5 μm after polishing. The wire was cut into segments with the length of 1 cm. The wires were sterilized by ultraviolet radiation overnight prior to surgery.

2.2. Ex vivo model – a vascular bioreactor

The protocols for collecting aortas were taken from the international guidelines on animal experiments, and approved by Institutional Animal Care and Use Committee (IACUC). One-year old mixed Danish Landrace and Yorkshire pigs weighing approximately 200 kg were obtained from Piedmont Custom Meats (former Matkins meat processors, Gibsonville, NC, USA). The porcine abdominal aortas were immediately collected from the slaughtered pigs and perfused by phosphate buffer solution to remove the blood. The aortas were immediately stored in Dulbecco's modified Eagle's medium (DMEM, Lonza®, USA) supplemented with 10% fetal bovine serum (FBS) and 1% penicillin-streptomycin (PS). The aortas were cut into segments with the length of 5 cm. All the aortas were maintained on ice before use.

The LumeGen bioreactor (TGT DynaGen® Series, USA) was chosen to provide a controllable environment for simulating physiological aortic conditions. The bioreactor consisted of blood-vessel chambers, variable-flow pump, hertz oscillator, flow control channel, culture medium, reservoir and incubator (Fig. 1a). A schematic diagram of the bioreactor system is shown in Fig. 1b. The entire system was sterilized by autoclavation.

Two Mg wires with the length of 1 cm were implanted into one aorta at two different positions (one exposed to the lumen and the other embedded in the wall) introduced by a syringe needle. The two implanted positions should simulate the stent surrounding environment at the early- and long-term implantation, respectively. A single aorta with two Mg wires was installed into each chamber (Fig. 1c), and the fluid through each aorta was from one reservoir (500 ml). DMEM with 10% FBS and 1% PS was chosen as a pseudo-physiological medium. The pH value of the solution was adjusted to 7.40 ± 0.05 prior to the test. Each chamber was filled with medium to a volume of 50 ml. The flow rate of the circulating medium was set to 100 ml/min. The luminal pressure oscillated in a range from 80 to 120 mmHg with a pulse frequency of 1 Hz, thus diastolic and systolic status of the aorta was simulated under the flow condition (Seen in Supplementary Video 1 and Fig. S1). As a control, another aorta with two Mg segments also was immersed into the chamber with static medium. Then, the setup was kept in the incubator at 37 °C and 5% CO_2 for 5 days. The culture medium was refreshed at the 3rd day, reproducing standard culture conditions. At 3rd and 5th day, all the samples were delicately removed from the bioreactor and transferred into a 5 ml centrifuge tube with DMEM for further analysis of the degradation behavior. Then, the aortas were fixed in 4% paraformaldehyde solution (Affymetrix USB

199431LT) overnight for histological assessment. The number of repetitive aortas at the dynamic and static conditions was three, respectively.

2.3. In vivo model – rat abdominal aorta

Comparative *in vivo* experiments were performed. For practical and ethical reasons, rats instead of pigs were selected as animal model in the *in vivo* test. Although the switch of animal model is a limitation of the study, the blood pressure in rats and pigs is comparable about 100 mmHg systolic and also the shear stresses in the arteries of small rodents are similar to those in big animals [24]. Therefore it is assumed that the here relevant diffusion properties of the tissues are also comparable.

The use of experimental animals was approved by the Animal Experiments Ethical Committee of Nankai University and carried out in conformity with the Guide for Care and Use of Laboratory Animals. Twelve 3-month-old female Sprague–Dawley rats weighing 300–350 g were anesthetized with chloral hydrate (300 mg/kg) by intraperitoneal injection. Heparin (100 units/kg) was administered for anticoagulation by tail vein injection before surgery. A midline laparotomy incision was then performed and the abdominal aorta with a diameter of 1.2 ± 0.2 mm was isolated, and clamped. The two sterilized Mg wire segments with the length of 1 cm were introduced into the wall and lumen of abdominal aorta by a syringe needle (Fig. 2). Gentamicin was injected into the abdomen prior to postoperative suture.

The 12 rats were sacrificed by injection of an overdose of chloral hydrate at the predetermined time points (the 3rd and 5th day). The abdominal aortas with the implanted wires were harvested for analysis. All the samples were fixed with 4% paraformaldehyde. Then, six samples were embedded in optimal cutting temperature compound (OCT, Fisher Healthcare™ Tissue-Plus™) for histological assessment. The other six samples were dehydrated and then used for degradation analysis. A dehydrating process was performed by immersion in 70%, 80%, 90% and 100% ethanol solution for 5 min, sequentially.

2.4. In vitro model – standard immersion

A Mg wire with the length of 1 cm was immersed into the chambers with static DMEM containing 10% FBS and 1% PS under cell culture conditions (37 °C, 5% CO_2) for 3 and 5 days [25]. The degradation behavior of the wires was analyzed after the test. Three independent wires were incubated and analyzed as repeats.

2.5. Degradation characterization

The appearances and cross-sectional images of the samples were analyzed by micro X-ray computed tomography (CT, GE Phoenix Nanotom-M™, GE Sensing & Inspection Technologies GmbH) at settings of 80 keV and 80 μA current. The *ex vivo* samples were tested in ethanol without dehydration, and the *in vivo* samples were tested in air after dehydration. Two-dimensional (2-D) planes and the three-dimensional (3-D) models were reconstructed using the Phoenix datos|x software. The volume ratio of residual Mg to the initial Mg, and the volume ratio of degradation products to residual Mg were calculated from CT data analysis using VG Studio Max software (v 2.1). Degradation rates (mm/y)

were calculated, but it should be noted that localized degradation was not taken into account and therefore the calculated degradation rates were rough estimates. The calculation of the degradation rates was based on the decrease of the metallic volume during the test period calculated from the obtained 3-D data. Assuming uniform degradation, the reduction of the implant volume could be converted into a degradation rate by using a modification of Eq. (1) [10]:

$$\mathrm{CR}=\frac{\Delta V}{At} \quad (1)$$

where CR represents degradation rate, ΔV is the volume loss which is equal to the difference between initial and residual volume of Mg metal, A is the implant surface area and t is the exposure time.

After the test, the samples were replaced to a chamber with new medium. The 5-day samples were used to analyze the chemical compositions of the degradation products using a field emission scanning electron microscope (SEM, SU8000, Hitachi, Japan) and electron dispersive X-ray spectroscopy (EDX, Bruker AXS5350, Germany) after sputter coating. The samples for cross sectional investigation of degradation products were prepared through polishing after mounting with epoxy resin (Epokwick® Epoxy resin, Buehler, USA).

2.6. Histology

Axial sections (10 μm in thickness) of the *ex vivo* and *in vivo* aortas embedded in OCT were cut in cryostat and then stained with Hematoxyline-Eosin (H&E, Surgipath®, Leica biosystems) for cytology images and von Kossa (von Kossa stain kit, American Master-Tech Scientific) for the localization of calcium phosphate crystals in the 3rd day and 5th day samples. Images were observed under an inverted microscope (cellSens, Olympus, Japan) and analyzed by cellSens software.

2.7. Statistical analysis

Statistical analysis was performed using Statistic Package for Social Science (SPSS, version 17). One-way analysis of variance (ANOVA) was conducted to test average degradation rate. Significance was established by a value of $p < 0.05$. Data are expressed as mean ± standard deviation (SD).

3. Results and discussion

3.1. Model rationale

Compared with the standard *in vitro* immersion test, the *ex vivo* vascular bioreactor provides biological, biophysical and biochemical factors that further simulate physiologically realistic vessel environments. In the biological view, the choice of porcine abdominal aorta is to provide a highly interactive three-dimensional (3-D) microenvironment composed of medium-material, material–cell, medium–cell, and cell–matrix interactions. These 3-D vascular tissue surroundings, allow more realistic degradation behavior and cellular responses than traditional 2-D culture.

From the biophysical view, the aorta in the bioreactor can keep the integrated vascular structure at a biologically active level, as shown in H&E images (Fig. 3 c–e). The arterial wall as a permeable channel, commonly consists of six layers: glycocalyx, endothelium, intima, internal elastic lamina, media, and adventitia [26,27]. One of the two Mg wire segments was exposed to the lumen and contacted the circulating medium and the endothelium (Fig. 3 d), simulating an early-term implantation environment. The other Mg wire was firmly embedded into the wall near the endothelium (Fig. 3 e), mimicking a long-term implantation environment. To simulate both of the early- and long-term environments, the Mg wires were used in all stages of the study to get more quantitative results instead of stents, since the same geometry of the implants can be implanted in the lumen and in the wall, which would not be possible with a stent. In terms of hemodynamics, this model can provide fluid shear induced by flow in the vessel, the tangential force derived from the friction of flowing across the luminal cell surface, tensile stress due to deformation of the vessel wall by transvascular flow, and normal stress caused by the hydrodynamic pressure differential across the vessel wall. As a result, flow became a dominating driving force on the degradation of the Mg wire exposed to the lumen, as well as fluid diffusion became a dominating driving force on the degradation of the Mg wire embedded in the wall. To understand the effects of fluid flow and diffusion, controls were prepared with the Mg wires in the aorta immersed in the media statically without flow.

From a biochemical point of view, DMEM with 10% FBS and 1% PS, as a pseudo-physiological medium, is much closer to blood content than other commonly used media (e.g. Hank's solution [28], Phosphate buffer saline [29], simulated body fluid [30]) in standard immersion tests. Moreover, flow diffusion improves the local tissue environment by inhibiting pH increase and metallic ion accumulation that may lead to cell death. However, of course compared to the *in vivo* situation, blood cells are missing in the *ex vivo* flow system and also the pH buffer capacity of the DMEM may be different than that of blood.

Besides the *ex vivo* condition of the vascular bioreactor, a Mg wire was immersed in the static solution without the effects of both aorta and flow as a traditional *in vitro* immersion control. As an *in vivo* control, two Mg wires were implanted into the rat abdominal aorta and the implanted positions were similar to that of the *ex vivo* test (Fig. 3 b). After 5 days, the rat aorta preformed a native pulsation status, illustrating blood stream (Seen in Supplementary Video 2). The study has a preliminary character, as we used different animal models: 1) porcine aorta artery for *ex vivo* bioreactor and 2) rat aorta artery model for the *in vivo* study. However, both experiments provided a comparison of Mg wire degradation rates, products, degradation types in two different positions (one in wall and one exposed to lumen). Due to the comparable blood pressure and vascular shear rates in both species, also similar diffusion and mass transport in the vessel wall of both species is assumed. Overall, the degradation behaviors of Mg were compared in all the *in vitro, ex vivo* and *in vivo* tests.

3.2. Degradation rates

Macroscopic 2-D and 3-D degradation morphologies were collected from X-ray CT data of the samples under each condition at the 3rd day (Fig. 4) and 5th day (Fig. S2) culture time. The average degradation rates (Table 1) were calculated based on the CT data according to

Eq. (1). Degradation rates of Mg showed no significant difference between the *in vitro* static condition, as well as the wall positions *ex vivo* and *in vivo* ($P > 0.1$), which are conditions, where diffusion controls the ion transport. Degradation rates of Mg at this diffusion condition correlate well among *in vitro, ex vivo*, and *in vivo* results. But at the lumen positions the degradation rates *ex vivo* and *in vivo* were significantly different ($P < 0.05$). Mg degradation at the lumen *ex vivo* was faster than that at the same position *in vivo*.

The degradation of the Mg wire embedded in the wall depends on the diffusion of water, solutes and ions, which pass inter-endothelial junctions by way of transportation utilizing fenestral pores embedded throughout the intima, internal elastic lamina, and media sections of the arterial wall [18]. The molecular diffusion within the arterial wall is driven by concentration gradients. A similar diffusion microenvironment at the wall positions *ex vivo* and *in vivo* conditions caused similar degradation rates of Mg. This slow diffusion microenvironment is very close to the static incubation condition. As a result, the degradation rates of Mg showed no significant difference at the *in vitro* static condition, as well as the wall positions *ex vivo* (static and dynamic) and *in vivo*.

However, the different degradation rates of Mg at the lumen positions between static *ex vivo*, dynamic *ex vivo* and *in vivo* conditions can be attributed to the different microenvironment and hydrodynamics. Compared with static *ex vivo* degradation, Mg degradation in the dynamic flow condition was significantly faster ($P < 0.05$). This is attributed to the fact that the flow accelerated the arrival of the corrosive medium with chloride ions to the Mg surface and removed the corrosion products [31]. Furthermore, mass transfer across the arterial wall occurs via two mechanisms: the pressure-driven transmural flow and diffusion caused by concentration gradients. In particular, mass transfer was accelerated by high mechanical force from flow-induced shear stress as well as pulsatile diastolic and systolic stress (Seen in Supplementary video) [16]. Also the soluble degradation products were removed faster in the dynamic flow condition, then fresh metal surfaces were exposed to the media. Additionally, there is always a steep concentration gradient around the degradation interface, that is, alkaline pH is rapidly refreshed by circulating medium. The fresh metal surface and medium replacement promoted degradation [32]. Because of the fast degradation, the part of the Mg that exposed to the lumen fractured at the 3rd day (Fig. 4), and disappeared at the 5th day under the continuous flow (Fig. S2). Different from intraluminal results *ex vivo*, the degradation rate of Mg wire in the lumen *in vivo* was significantly lower, even it was a little slower than that in the wall of *in vivo* aorta model (Fig. 4). This is consistent with a previous report by Pierson et al. in the case of iron wires for 9 months [33]. We observed that a fibrous capsule *in vivo* integrally covered on the Mg surface in the lumen for 3 days (Fig. 5). Thus Mg degradation occurred under diffusion control instead of flow, slowing down the degradation rate. More discussions can be found in the following Section 3.3.

In general, a lower degradation rate was observed *in vivo* compared with *in vitro* and *ex vivo*. One possible explanation is that the degradation rate relies heavily on the degradation media. Sanchez et al. reported that the degradation of Mg materials in minimum essential medium is 1.5–3.5 times as high as *in vivo*. The addition of proteins increased this value to a range between 4 and 7 times [7]. Additionally, there is lower concentration of chloride (Cl^-) ions present in blood plasma (103 mM) [7,34] than in DMEM (118 mM). The Cl^- ion is an

aggressive factor on the acceleration of the Mg degradation [17,35]. Another possible explanation for the lower degradation rate obtained *in vivo* is the response of the host tissue to the surgical procedure and the presence of the material (e.g. inflammation and foreign body reaction): an initial pH decrease directly after surgery can result in a short-term enhancement of the degradation rate, with the consequent formation of a stable degradation layer, which reduces the subsequent degradation rate of the implants [10]. In addition, more complex biological factors including cellular (e.g. immune cells) and molecular factors (e.g. integrins) are involved *in vivo*.

3.3. Degradation products

The formation, evolution and degradation of degradation products play a vital role on the fate of Mg implants. The distribution of degradation products on the Mg surface were analyzed by X-ray CT and marked yellow in the 2-D sections in Figs. 4 and S2. More degradation products accumulated on the Mg surface in the static conditions compared with the dynamic conditions. To analyze the degradation more accurately, the volumes of the degradation products and the residual Mg were calculated based on the CT data, respectively (Fig. 6). The volume ratios of residual Mg can be defined as the residual Mg volume divided by the initial volume. Also, the volume ratio of degradation products can be defined as the degradation products volume divided by the initial sample volume. The degradation products deposit much easier under static than under flow conditions. With the evolution of the degradation over time, the amount of degradation products slightly increased at the *in vitro* and *ex vivo* conditions. However, the increase in degradation and its products was not obvious from 3rd day to 5th day at the *in vivo* conditions. It indicates that the degradation changes very slowly once a degradation product layer is formed, as well as the degradation products layer is relatively stable *in vivo*.

Von Kossa silver staining, which is sensitive for calcium- and magnesium-phosphate precipitates were [36] was used to further analyze the distribution of the degradation product particles in the tissue (Fig. 5). Most precipitates were found for the *ex vivo* dynamic condition, followed by the *ex vivo* static condition. In general there were more precipitates for the lumen implants than for the aorta wall implants. The phosphate salt precipitates thus correlate well with the observed corrosion products observed in CT. Moreover, a thicker and denser fibrous capsule was found around the Mg wire at the lumen position *in vivo* after 3 days, and the Mg wire was covered by neointima after 5 days (Fig. 5). This provided a fluid diffusion control and prevented fluid flow and flow-induced shear stress on the Mg surface, which contributed to the slower degradation rate and less degradation product particles at the intra-luminal condition *in vivo*, compared with intra-luminal condition *ex vivo*. The diffusion control by the capsule also maintained a higher pH around the implant. Bartsh et al. [37] were able to prove the existence of the alkaline milieu near implanted Mg material in living immunocompetent mice by *in vivo* fluorescent image. The high pH microenvironment alleviated the degradation [17].

The chemical compositions of the degradation products on the cross-sections of the samples were analyzed using EDX mapping (Fig. 7). The elemental distributions of degradation product layers consisted of two layers, a main outer layer composed of Ca, P and O and a

very thin inner layer composed of Mg and O, as previously reported [38]. The Mg-rich and O-rich layers were composed of MgO and/or $Mg(OH)_2$ [39]. The MgO and/or $Mg(OH)_2$ layer is not obviously between the metal and product interface. According to the E-pH diagram (Pourbaix diagram) [40], there should be no $Mg(OH)_2$ layer on a magnesium surface in a solution with a pH lower than 10.5 because $Mg(OH)_2$ is not stable under such conditions (the pH value required for the precipitation of $Mg(OH)_2$ is around 10.5). The P-rich, Ca-rich and O-rich zones for all samples suggested that there was a formation of a calcium phosphate (Ca-P) layer on the Mg surface [25]. The formation of Ca-P was caused by the precipitation of the Ca^{2+} and HPO_4^{2-} from DMEM, blood or tissue, which can commonly be found in biomineralization [25]. The depositions of Ca-P were more pronounced at the *in vitro* and *ex vivo* conditions than *in vivo* conditions (Fig. 7). The fast Mg degradation in the first two conditions, associated with pH shifts promoted the Ca-P precipitation [16], whereas the slow degradation rate *in vivo* also caused only slow accumulation of Ca-P. The degradation product layer was more uniform and dense *in vivo* than at the other conditions. Thus, this layer, as a passivation layer, decreased the degradation rate *in vivo*.

3.4. Degradation modes

The degradation modes of Mg implants at each condition were analyzed by X-ray micro-CT 2-D slices in Fig. 8. Based on the degradation morphologies, the test conditions mainly affected two modes of degradation, localized and uniform degradation. The corrosion mode in the standard static *in vitro* assay was highly localized; the *ex vivo* model produced less localized and more uniform corrosion; this better resembled the *in vivo* corrosion, which was highly uniform. One proposed reason (albeit tentative) is the suppression of localized degradation *in vivo*, possibly due to the encapsulation of the material by the surrounding tissues [41]. In particular, a large amount of solid degradation products were found inside the localized degradation areas of the Mg implant at the *in vitro* and *ex vivo* conditions (Figs. 8 and S3). A thin and uniform degradation product layer covered on the surface of the Mg implant *in vivo* as shown in EDX data (Fig. 7). Of particular interest are some small gas cavities, which are easy to observe around the localized degradation areas of the Mg implant in the *ex vivo* condition. Hydrogen is a main gaseous degradation product from Mg degradation. A remarkable amount of hydrogen is ascribed to the fast degradation inside the localized degradation areas and the diffusion and solubility of hydrogen gas is limited in the tissue, causing the bubble formation. This phenomenon is hard to find *in vitro*. The positions of gas accumulation will become potential fracture points in the Mg due to the hydrogen embrittlement [42].

There are some limitations in the current *ex vivo* vascular bioreactor model. (1) Although the aorta (Fig. 3) in the bioreactor chamber was maintained at a biologically active level, endothelialization could not be mimicked at the *ex vivo* condition. Abundant proteins and a fibrous capsule rapidly covered the Mg implants *in vivo*, which was not simulated at the current *ex vivo* model either. (2) Different flow rate and size of the porcine versus rat aorta *ex vivo* and *in vivo*, respectively, make direct comparison between the bioreactor and *in vivo* implantation model difficult. (3) The geometry of the stent and supporting force should affect degradation, which have not considered in this study. If these problems are solved,

there will be better understanding about discrepant Mg biodegradation rates and modes *in vivo* and in *in vitro* tests.

4. Conclusion

An *ex vivo* vascular bioreactor was developed to mimic *in vivo* microenvironment with comprehensive parameters to study biodegradation behavior of Mg implants. Considering hemodynamics and microenvironment around the stent at the early- and long-term implantation process, we investigated the Mg degradation behavior in an aortic lumen and wall with incubation in a bioreactor under static and dynamic conditions. This was compared with the implantation in the aortic lumen and wall *in vivo* and the static immersion *in vitro* without aorta. The degradation rates on the diffusion models (i.e. *in vitro* static condition, the aortic wall positions of *ex vivo* and *in vivo* conditions) were not significantly different. But Mg degradation at the fluid flow condition (i.e. lumen) *in vivo* was slower than that *ex vivo*. This is attributed to the synergistic effects on mass transfer, ion exchange, fluid flow and diffusion, as well as response of the host tissue. The corrosion mode in the standard static *in vitro* assay was highly localized; the *ex vivo* model produced less localized and more uniform corrosion; this better resembled the *in vivo* corrosion, which was highly uniform. The abundant degradation products accumulated inside the spots of localized degradation *in vitro* and *ex vivo*; however, the uniform product layer dominated at the *in vivo* condition. Hydrogen bubbles occurred around the localized degradation regions *ex vivo* due to diffusion limited areas in the tissue. In addition, the deposition of Ca-P degradation product to tissue depended on the Mg degradation rate. For successful *in vitro* testing of absorbable Mg-based stents, biodegradation conditions still need to be improved for screening the degradation rates of new Mg-based stents *in vitro* and to understand the mechanisms of biodegradation.

Supplementary Material

Refer to Web version on PubMed Central for supplementary material.

Acknowledgments

This study was supported by the Engineering Research Center for Revolutionizing Metallic Biomaterials (NSF-0812348) from the National Science Foundation, USA; NIH NIGMS SCORE Grant (1SC3GM113728-01), USA; National Natural Science Foundation of China under Grant No. 81330031, No. 31600766 and No. 21473138; Fundamental Research Funds for the Central Universities under Grant No. 2682016CX076; and X-ray CT imaging was made possible through an USA-NSF Award No. 0959511.

Appendix A. Figures with essential colour discrimination

Certain figures in this article, particularly Figs. 1–8 are difficult to interpret in black and white. The full colour images can be found in the on-line version, at doi: 10.1016/j.actbio.2016.12.039.

Appendix B. Supplementary data

Supplementary data associated with this article can be found, in the online version, at http://dx.doi.org/10.1016/j.actbio.2016.12.039.

References

1. Zheng YF, Gu XN, Witte F. Biodegradable metals. Mater Sci Eng R. 2014; 77:1–34.
2. Witte F. The history of biodegradable magnesium implants: a review. Acta Biomater. 2010; 6:1680–1692. [PubMed: 20172057]
3. Feyerabend F, Wendel HP, Mihailova B, Heidrich S, Agha NA, Bismayer U, Willumeit-Romer R. Blood compatibility of magnesium and its alloys. Acta Biomater. 2015; 25:384–394. [PubMed: 26210283]
4. Yang L, Hort N, Willumeit R, Feyerabend F. Effects of corrosion environment and proteins on magnesium corrosion, Corros. Eng Sci Technol. 2012; 47:335–339.
5. Waksman R, Erbel R, Di Mario C, Bartunek J, de Bruyne B, Eberli FR, Erne P, Haude M, Horrigan M, Ilsley C, Bose D, Bonnier H, Koolen J, Luscher TF, Weissman NJ, P.-A. Investigators. Early- and long-term intravascular ultrasound and angiographic findings after bioabsorbable magnesium stent implantation in human coronary arteries, JACC Cardiovasc. Interventions. 2009; 2:312–320.
6. Haude M, Erbel R, Erne P, Verheye S, Degen H, Böse D, Vermeersch P, Wijnbergen I, Weissman N, Prati F, Waksman R, Koolen J. Safety and performance of the drug-eluting absorbable metal scaffold (DREAMS) in patients with de-novo coronary lesions: 12 month results of the prospective, multicentre, first-in-man BIOSOLVE-I trial. Lancet. 2013; 381:836–844. [PubMed: 23332165]
7. Sanchez AHM, Luthringer BJC, Feyerabend F, Willumeit R. Mg and Mg alloys: how comparable are in vitro and in vivo corrosion rates? A review. Acta biomaterialia. 2015; 13:16–31. [PubMed: 25484334]
8. ISO/TS 17137: 2014(E). Cardiovascular implants and extracorporeal systems—Cardiovascular absorbable implants. 2014
9. Kirkland NT, Birbilis N, Staiger MP. Assessing the corrosion of biodegradable magnesium implants: A critical review of current methodologies and their limitations. Acta Biomater. 2012; 8:925–936. [PubMed: 22134164]
10. Witte F, Fischer J, Nellesen J, Crostack HA, Kaese V, Pisch A, Beckmann F, Windhagen H. In vitro and in vivo corrosion measurements of magnesium alloys. Biomaterials. 2006; 27:1013–1018. [PubMed: 16122786]
11. Wang J, Smith CE, Sankar J, Yun Y, Huang N. Absorbable magnesium-based stent: physiological factors to consider for in vitro degradation assessments. Regener Biomater. 2015:rbu015.
12. Shaw B, Wolfe R. Corrosion of magnesium and magnesium-base alloys. ASM Handbook. Corros Mater. 2005; 13:205–227.
13. Jang Y, Collins B, Sankar J, Yun Y. Effect of biologically relevant ions on the corrosion products formed on alloy AZ31B: an improved understanding of magnesium corrosion. Acta Biomater. 2013; 9:8761–8770. [PubMed: 23535231]
14. Wang J, Witte F, Xi T, Zheng Y, Yang K, Yang Y, Zhao D, Meng J, Li Y, Li W, Chan K, Qin L. Recommendation for modifying current cytotoxicity testing standards for biodegradable magnesium-based materials. Acta Biomater. 2015; 21:237–249. [PubMed: 25890098]
15. Erbel R, Di Mario C, Bartunek J, Bonnier J, de Bruyne B, Eberli FR, Erne P, Haude M, Heublein B, Horrigan M, Ilsley C, Böse D, Koolen J, Lüscher TF, Weissman N, Waksman R. Temporary scaffolding of coronary arteries with bioabsorbable magnesium stents: a prospective, non-randomised multicentre trial. Lancet. 2007; 369:1869–1875. [PubMed: 17544767]
16. Wang J, Giridharan V, Shanov V, Xu Z, Collins B, White L, Jang Y, Sankar J, Huang N, Yun Y. Flow-induced corrosion behavior of absorbable magnesium-based stents. Acta Biomater. 2014; 10:5213–5223. [PubMed: 25200844]
17. Zhao MC, Liu M, Song GL, Atrens A. Influence of pH and chloride ion concentration on the corrosion of Mg alloy ZE41. Corros Sci. 2008; 50:3168–3178.
18. Wang J, Smith CE, Sankar J, Yun Y, Huang N. Absorbable magnesium-based stent: physiological factors to consider for in vitro degradation assessments. Regener Biomater. 2015; 2:59–69.
19. Willumeit R, Feyerabend F, Huber N. Magnesium degradation as determined by artificial neural networks. Acta Biomater. 2013; 9:8722–8729. [PubMed: 23470548]

20. Wang, J. PhD thesis. Southwest Jiaotong University; 2015. Biodegradation Behavior and Biological Responses of Magnesium-based Materials for Vascular Stents in the Hydrodynamic Near-Physiological Ambient Conditions.
21. Lévesque J, Hermawan H, Dubé D, Mantovani D. Design of a pseudo-physiological test bench specific to the development of biodegradable metallic biomaterials. Acta Biomater. 2008; 4:284–295. [PubMed: 18033745]
22. Di Mario C, Griffiths HUW, Goktekin O, Peeters N, Verbist JAN, Bosiers M, Deloose K, Heublein B, Rohde R, Kasese V. Drug-eluting bioabsorbable magnesium stent. J Interventional Cardiol. 2004; 17:391–395.
23. Heublein B, Rohde R, Kaese V, Niemeyer M, Hartung W, Haverich A. Biocorrosion of magnesium alloys: a new principle in cardiovascular implant technology? Heart. 2003; 89:651–656. [PubMed: 12748224]
24. Suo J, Ferrara DE, Sorescu D, Guldberg RE, Taylor WR, Giddens DP. Hemodynamic shear stresses in mouse aortas implications for atherogenesis. Arterioscler Thromb Vasc Biol. 2007; 27:346–351. [PubMed: 17122449]
25. Willumeit R, Fischer J, Feyerabend F, Hort N, Bismayer U, Heidrich S, Mihailova B. Chemical surface alteration of biodegradable magnesium exposed to corrosion media. Acta Biomater. 2011; 7:2704–2715. [PubMed: 21382530]
26. Khakpour M, Vafai K. Critical assessment of arterial transport models. Int J Heat Mass Transf. 2008; 51:807–822.
27. Yang N, Vafai K. Modeling of low-density lipoprotein (LDL) transport in the artery—effects of hypertension. Int J Heat Mass Transf. 2006; 49:850–867.
28. Ren Y, Huang J, Zhang B, Yang K. Preliminary study of biodegradation of AZ31B magnesium alloy. Front Mater Sci Chin. 2007; 1:401–404.
29. Gupta RK, Mensah-Darkwa K, Kumar D. Corrosion protective conversion coatings on magnesium disks using a hydrothermal technique. J Mater Sci Technol. 2014; 30:47–53.
30. Seitz JM, Collier K, Wulf E, Bormann D, Bach FW. Comparison of the corrosion behavior of coated and uncoated magnesium alloys in an in vitro corrosion environment. Adv Eng Mater. 2011; 13:B313–B323.
31. Ghali E, Dietzel W, Kainer KU. General and localized corrosion of magnesium alloys: a critical review. J Mater Eng Perform. 2004; 13:7–23.
32. Wang J, Jang Y, Wan G, Giridharan V, Song GL, Xu Z, Koo Y, Qi P, Sankar J, Huang N, Yun Y. Flow-induced corrosion of absorbable magnesium alloy: in-situ and real-time electrochemical study. Corros Sci. 2016; 104:277–289. [PubMed: 28626241]
33. Pierson D, Edick J, Tauscher A, Pokorney E, Bowen P, Gelbaugh J, Stinson J, Getty H, Lee CH, Drelich J, Goldman J. A simplified in vivo approach for evaluating the bioabsorbable behavior of candidate stent materials. J Biomed Mater Res B Appl Biomater. 2012; 100B:58–67.
34. Wills M, McGowan G. Plasma-chloride levels in hyperparathyroidism and other hypercalcaemic states. Br Med J. 1964; 1:1153–1156. [PubMed: 14120808]
35. Pardo A, Merino M, Coy AE, Arrabal R, Viejo F, Matykina E. Corrosion behaviour of magnesium/aluminium alloys in 3.5 wt.% NaCl. Corros Sci. 2008; 50:823–834.
36. Rajamannan NM, Subramaniam M, Rickard D, Stock SR, Donovan J, Springett M, Orszulak T, Fullerton DA, Tajik AJ, Bonow RO. Human aortic valve calcification is associated with an osteoblast phenotype. Circulation. 2003; 107:2181–2184. [PubMed: 12719282]
37. Bartsch I, Willbold E, Rosenhahn B, Witte F. Non-invasive pH determination adjacent to degradable biomaterials in vivo. Acta Biomater. 2014; 10:34–39. [PubMed: 24021229]
38. Bowen PK, Drelich J, Goldman J. Magnesium in the murine artery: probing the products of corrosion. Acta Biomater. 2014; 10:1475–1483. [PubMed: 24296127]
39. Mueller WD, Nascimento ML, De Mele MFL. Critical discussion of the results from different corrosion studies of Mg and Mg alloys for biomaterial applications. Acta Biomater. 2010; 6:1749–1755. [PubMed: 20051271]
40. Pourbaix M. Atlas of electrochemical equilibria in aqueous solutions. 1974

41. Abidin NIZ, Rolfe B, Owen H, Malisano J, Martin D, Hofstetter J, Uggowitzer PJ, Atrens A. The in vivo and in vitro corrosion of high-purity magnesium and magnesium alloys WZ21 and AZ91. Corros Sci. 2013; 75:354–366.

42. Stampella R, Procter R, Ashworth V. Environmentally-induced cracking of magnesium. Corros Sci. 1984; 24:325–341.

Statement of Significance

Magnesium and its alloys are candidates for a new generation of biodegradable stent materials. However, the *in vitro* degradation of magnesium stents does not match the *clinical* degradation rates, corrupting the validity of conventional degradation tests. Here we report an *ex vivo* vascular bioreactor, which allows simulation of the microenvironment with and without blood vessel integration to study the biodegradation of magnesium implants in comparison with standard *in vitro* test conditions and with *in vivo* implantations. The bioreactor did simulate the corrosion of an intramural implant very well, but showed too high degradation for non-covered implants. It is concluded that this system is in between static incubation and animal experiments concerning the predictivity of the degradation.

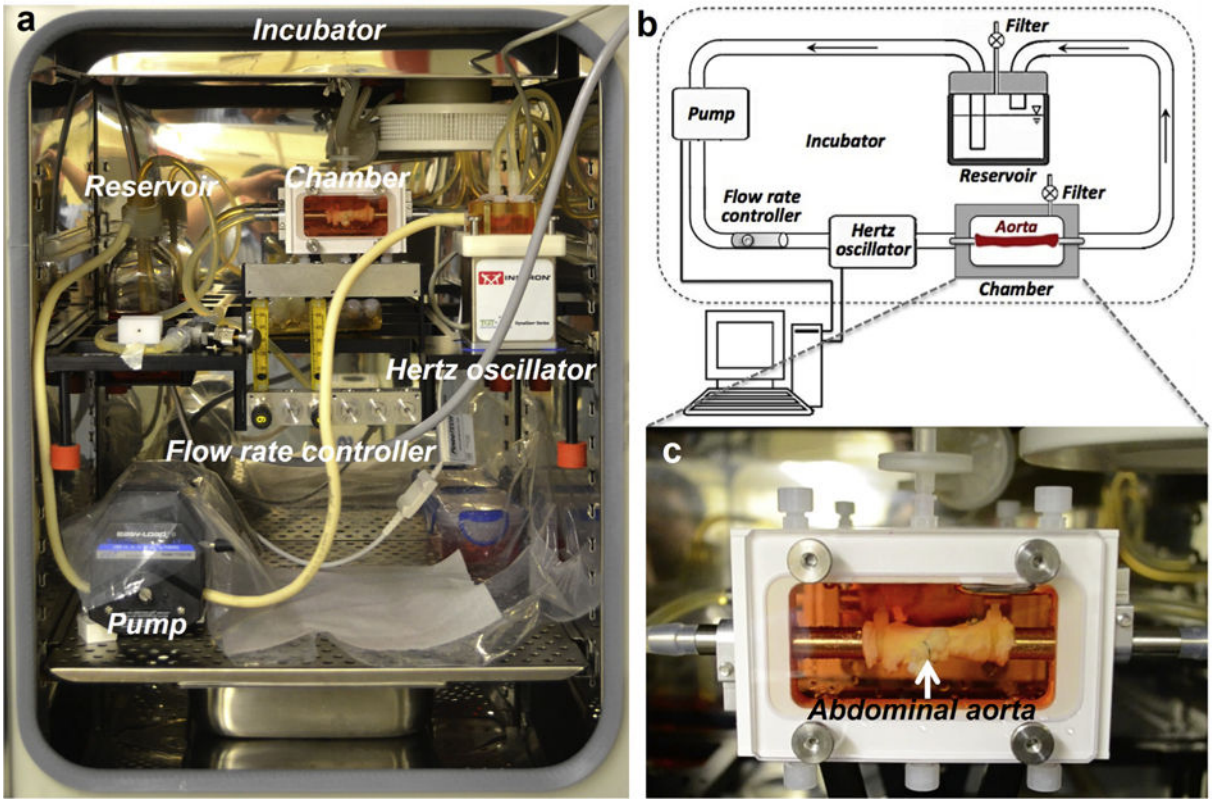

Fig. 1.

(a) Photographical image of the Lume Gen Bioreactor. (b) Schematic diagram of bioreactor system. (c) An aorta with two Mg wires implanted is mounted into the chamber.

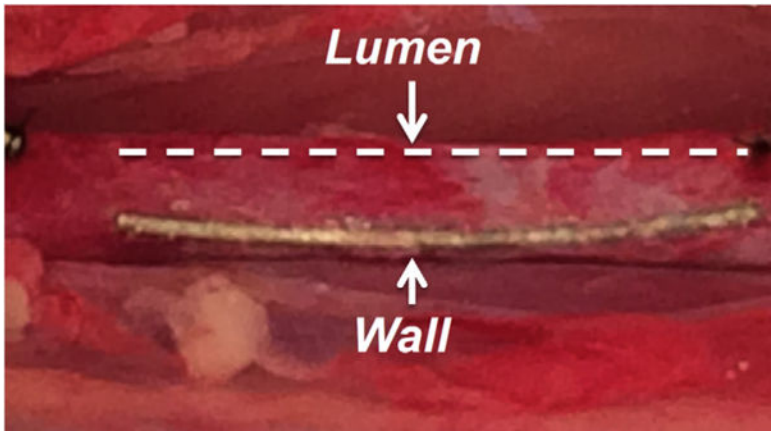

Fig. 2.
The two Mg wires implanted into a rat aorta wall and lumen. The dashes line marked the Mg wire implanted in the lumen.

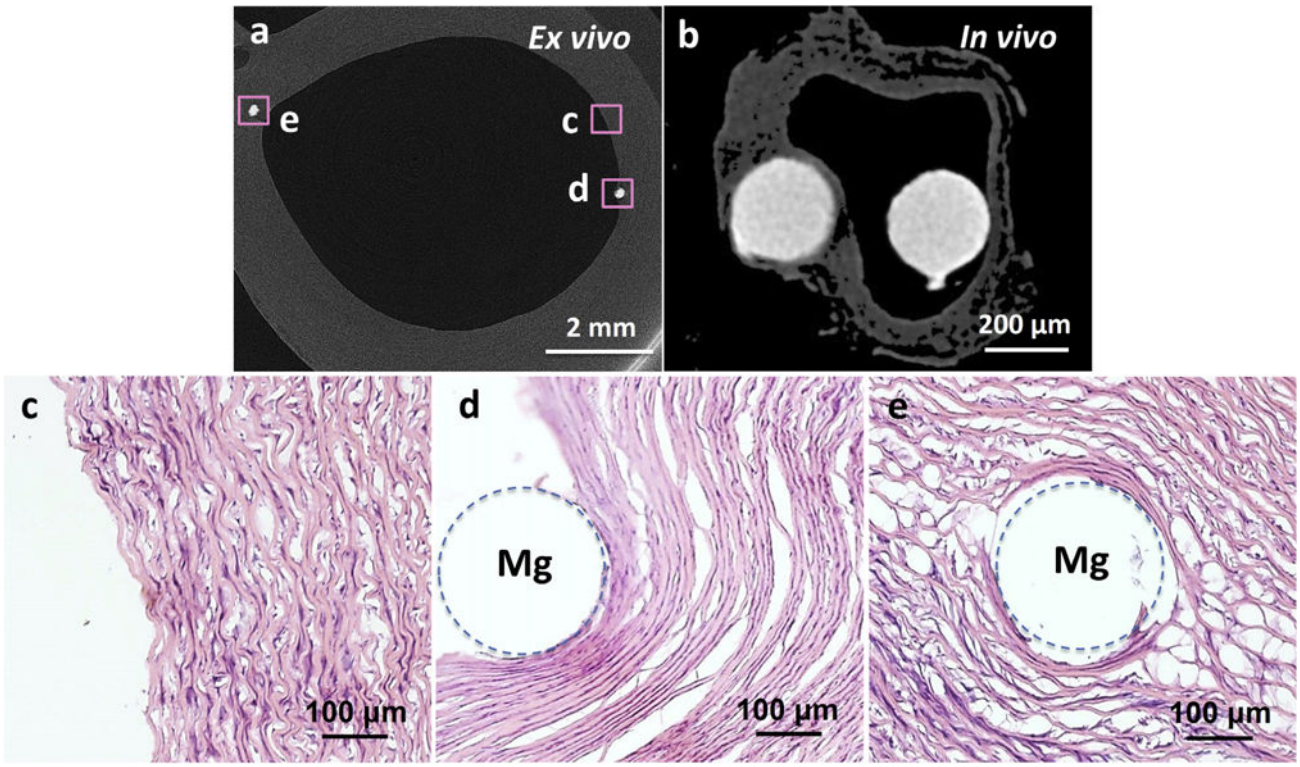

Fig. 3.

Typical implantation sites: Reconstruction of X-ray micro-CT 2-D cross-section slices of a porcine aorta with two Mg wires for the *ex vivo* vascular bioreactor test (a) and a dehydrated rat aorta with two Mg wires for the *in vivo* test (b). Mg wire on the left was under the intima and on the right was exposed to the lumen. H&E stain of an *ex vivo* control sample without implant (c), Mg wires implanted at the intraluminal (d) and wall (e) positions. Dashed circles show the positions of the Mg implants.

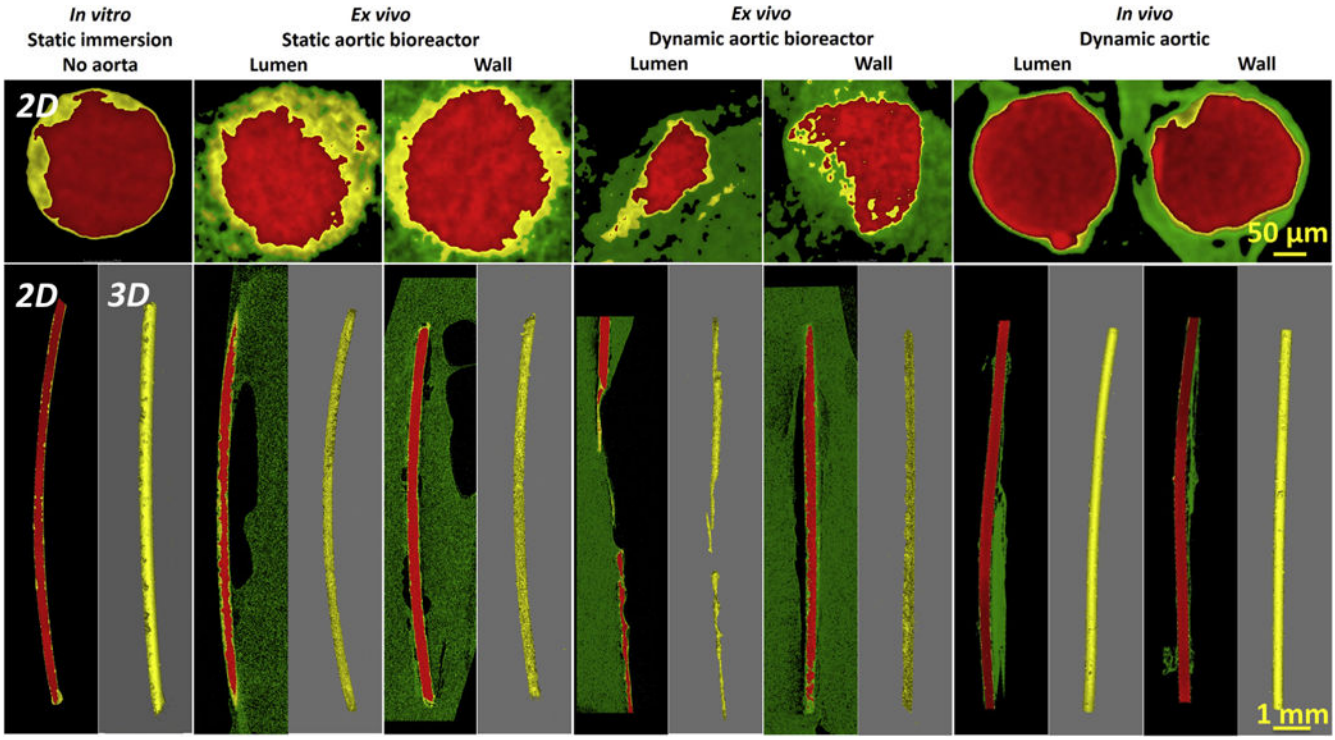

Fig. 4.

Reconstructions of X-ray micro-CT 3-D with representative 2-D slices of Mg wires under static incubation *in vitro* without aorta, static and dynamic incubation *ex vivo* in aortic lumen and wall in the bioreactors, and dynamic incubation in aortic lumen and wall *in vivo* after 3 days. The red parts represent Mg residual, the yellow parts represent degradation products, and the green parts represent host tissue. Note: There are no images for the dynamic *ex vivo* aortic lumen in the bioreactor, since no residual implant was left. (For interpretation of the references to colour in this figure legend, the reader is referred to the web version of this article.)

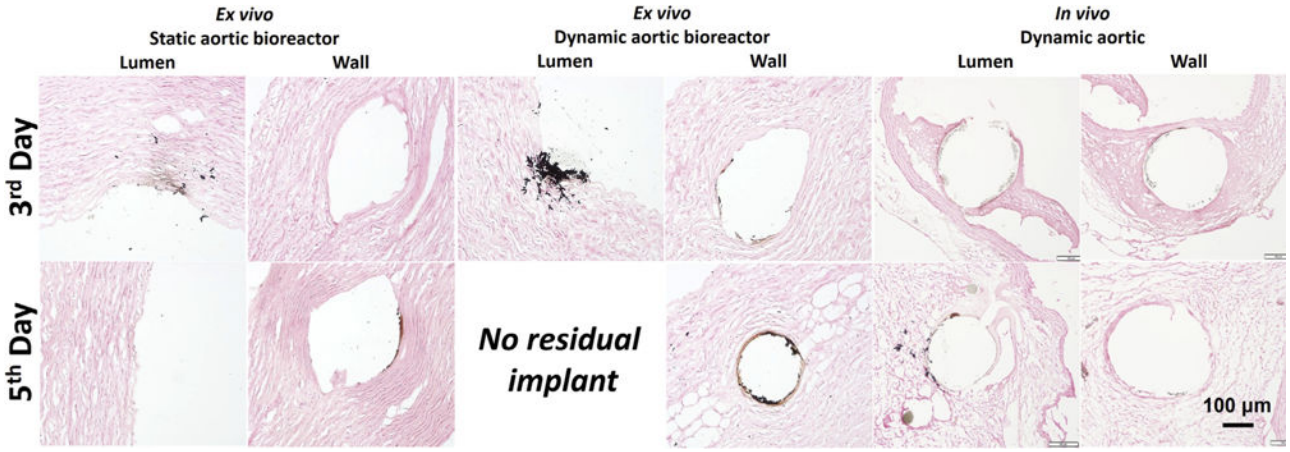

Fig. 5.

Von Kossa staining (dark brown indicates a positive stain) for Mg wires implanted the *ex vivo* static and dynamic aortic lumen and/or wall in the bioreactors and *in vivo* condition at 3rd day and 5th day.

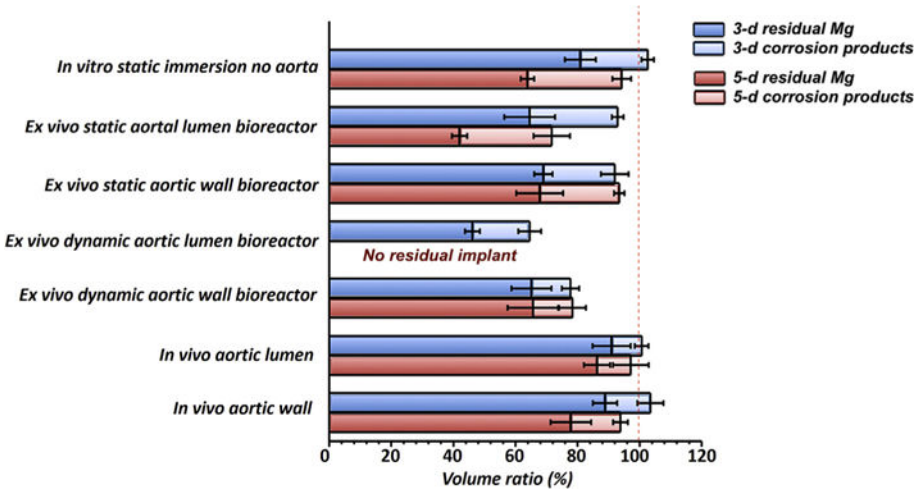

Fig. 6.

Volume ratios of residual Mg alloys and degradation products after 3 and 5 days obtained from the CT scans (Fig. 4). (Number of samples: N = 4).

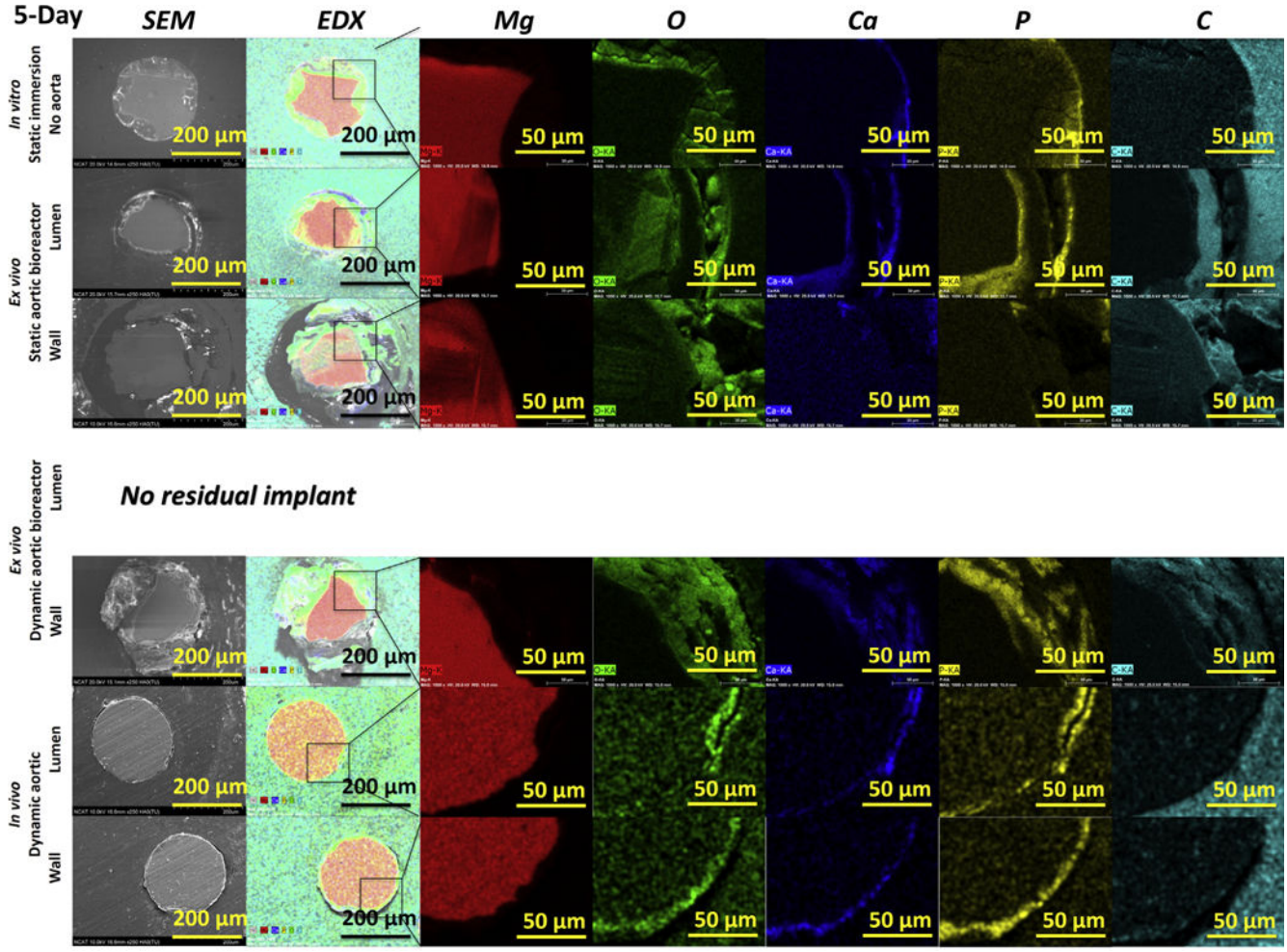

Fig. 7.

Cross-section SEM images with EDX mapping analysis of the samples after 5 days. No images exist for the dynamic *ex vivo* aortic lumen in the bioreactor, since no residual implant was left. Second column are EDX overlay images for the elements Mg (red), O (green), Ca (blue), P (yellow) and C (cyan), shown separately in the right columns. (For interpretation of the references to colour in this figure legend, the reader is referred to the web version of this article.)

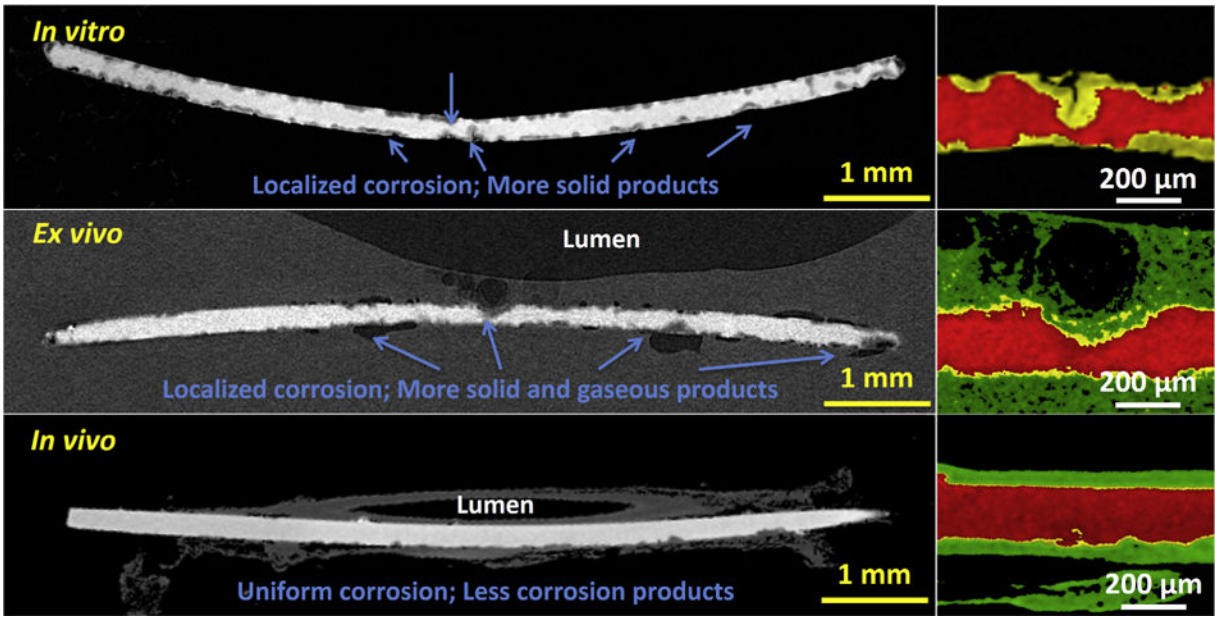

Fig. 8.

Typical reconstructions of X-ray micro-CT 2-D slices of Mg wires at the *in vitro, ex vivo* and *in vivo* conditions. Arrows indicate localized degradation areas and degradation products. The red parts represent residual Mg, the yellow parts represent degradation products, and the green parts represent tissue. (For interpretation of the references to colour in this figure legend, the reader is referred to the web version of this article.)

Table 1

Average degradation rates of Mg wires in the conditions of *in vitro* static immersion without aorta, *ex vivo* static and dynamic aortic lumen and wall in the bioreactors, and *in vivo* dynamic aortic lumen and wall.

Models	***In vitro*** **Static immersion**	***Ex vivo*** **Static aortic bioreactor**		***Ex vivo*** **Dynamic aortic bioreactor**		***In vivo*** **Dynamic aortic**	
Implanted position	**No aorta**	**Lumen**	**Wall**	**Lumen**	**Wall**	**Lumen**	**Wall**
Average degradation rate (mm/y)	1.6 ± 0.3	2.8 ± 0.4 *	1.8 ± 0.7	>4.0 ± 0.8 *	1.9 ± 0.5	1.1 ± 0.3 *	1.5 ± 0.6

* Represents significant differences between *ex vivo* static lumen, *ex vivo* dynamic lumen and *in vivo* lumen ($P < 0.05$).